

Simulation of cantilever beam micro-switch pull-in and collapse voltages

J.R. Reid and L.A. Starman

Air Force Research Laboratory, AFRL/SNHA
80 Scott Dr., Hanscom AFB, MA, USA, james.reid@hanscom.af.mil

ABSTRACT

Simulations of cantilever beam micro-switches exhibit two important operational voltages: the pull-in voltage when contact is initiated at the landing electrode; and the collapse voltage when the cantilever collapses onto the drive electrode. In between these two voltage levels is the operational range of the switch. Our simulations show that the operational range of the switch is heavily dependent on the switch design. As demonstrated here, increasing the electrode width decreases both the pull-in and collapse voltages. However, the percentage decrease in the pull-in voltage is well below that of the collapse voltage. Thus wider electrodes constrain the operating region of the switch.

Keywords: RF MEMS, Direct contact, Micro-switches, Cantilever.

1 INTRODUCTION

The design of direct contact (metal-metal) micro-switches is driven by the need to provide sufficient contact [1,2] and separation forces. For a fixed design such as that shown in Figure 1 the separation force is directly related to the pull-in voltage with a lower pull-in voltage resulting in a lower separation force. In addition, above the pull-in voltage, the applied force is directly proportional to the square of the applied voltage. Therefore, the maximum contact force is determined by the maximum voltage that can be applied before the cantilever collapses onto the control electrode. This paper presents a comparison of simulated pull-in and collapse voltages for electrostatically actuated cantilever micro-switches.

2 SIMULATION

2.1 MECHANICAL MODEL

The basic cantilever is shown in Figure 1 with an optical view shown in Figure 2. Across the width, the cantilever is considered to be uniform. Along the length, the beam is broken down into individual elements of equal length. Generally, 250 elements are used. Each element is allowed to move in only one dimension, up or down. This results in a quasi-two-dimensional model. It is assumed that the anchored end of the cantilever is

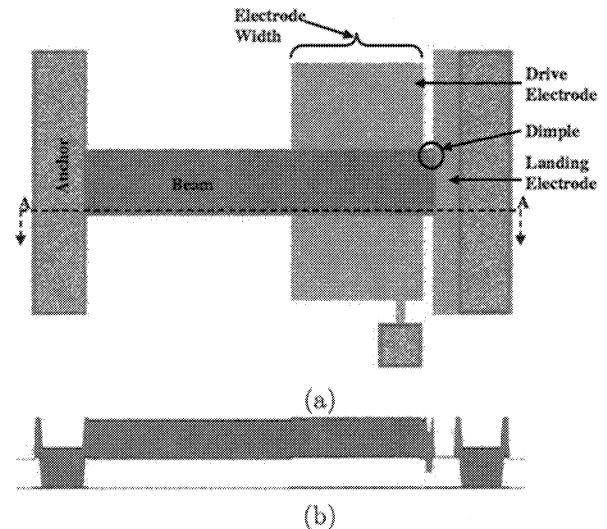


Figure 1: A direct contact cantilever beam switch. The switch is anchored at the left and extends out over the drive and landing electrodes. A bias is applied between the beam and the drive electrode to deflect the switch. Contact is initially made in the dimple regions between the beam and the landing electrode. The basic regions are illustrated in (a) and the cross section A-A of the switch is shown in (b).

rigidly clamped. Under the cantilever, the drive electrode provides a bias. For simulating contact force, an 'artificial' dielectric is placed on top of the electrode. This dielectric is considered to be impenetrable and is equivalent to the dimple height. The dielectric is set to have permittivity $\epsilon_r = 1$ so that it appears the same as air.

2.2 ELECTROSTATIC MODEL

Electrostatic calculations consist of determining the capacitance between the cantilever and the electrode, the charge density on the cantilever, the electric field generated by the electrode, and finally the force acting on the upper electrode. The parallel-plate approxima-

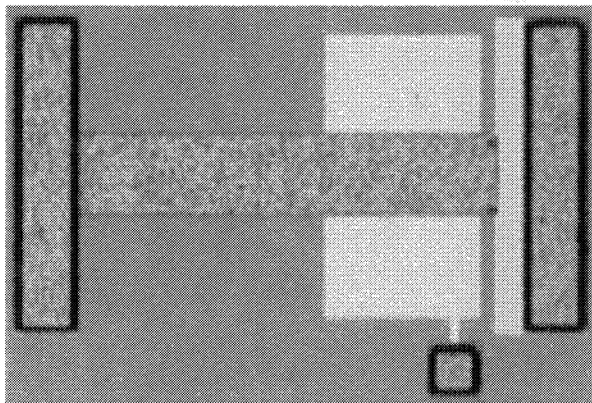


Figure 2: An optical picture of the device fabricated using gold metallizations on a gallium arsenide substrate. For this device, the beam is $75\ \mu\text{m}$ -wide, $400\ \mu\text{m}$ -long and is suspended $3\ \mu\text{m}$ above the substrate. The electrode width is $150\ \mu\text{m}$ and dimples are nominally $1.5\ \mu\text{m}$ deep.

tion is used to calculate the capacitance as

$$C_{seg} = \frac{\epsilon_0 W_{beam} L_{seg}}{x_{seg} + t_{die}} \quad (1)$$

where ϵ_0 is the permittivity of air, W_{beam} is the width of the cantilever, L_{seg} is the length of the individual segment, x_{seg} is the distance from the top of the dielectric to the cantilever at each segment, and t_{die} is the thickness of the 'artificial' dielectric. For typical cantilevers, the total overlap area is on the order of $50\ \mu\text{m}$ by $50\ \mu\text{m}$ with a separation of $3\ \mu\text{m}$ or less and thus the parallel plate approximation should introduce an error less than twenty percent, which decreases as the separation is reduced. This is sufficient for studying the switch operation, but more accurate models such as those described by Osterberg may be required to improve accuracy [3].

For each segment, the charge density is calculated as

$$\rho_{seg} = \frac{C_{seg} V_{bias}}{W_{beam} L_{seg}} \quad (2)$$

where V_{bias} is the potential applied to the drive electrode. The voltage-induced charge is positive for the beam and negative for the electrode. The field applied to the segment is calculated simply as $E_{seg} = V/2d$. Finally, the force is calculated as $F_{seg} = E_{seg} \rho_{seg} W_{beam}$.

2.3 DEFLECTION CALCULATION

Solving the deflection is done by assuming the cantilever has no internal stress. The deflection is then readily solved by a numerical implementation of the method of double integration as described in reference [4]. After the beam deflection is solved, the deflection

at the tip is checked to see if the tip has penetrated the dielectric. If the tip has penetrated the dielectric, a counter force is applied to the tip segment. This force is increased iteratively until the $x_{seg} = 0$, or the beam buckles. If buckling occurs, the tip segment of the beam is removed from the calculation and the process is repeated beginning with the deflection calculation. This is done until a valid solution is found. At this point, the entire calculation of charge, field, force, and deflection is repeated beginning with the beam having the calculated deflection. This process is repeated until the deflection calculations converge.

3 EXPERIMENTAL

A series of $75\ \mu\text{m}$ -wide by $400\ \mu\text{m}$ -long direct contact switches, as shown in Figure 1, were tested to characterize the pull-in and collapse voltages. The cantilever switches tested employed underlying drive electrode widths that varied from $50\ \mu\text{m}$ to $350\ \mu\text{m}$. The switch design consists of a $4\ \mu\text{m}$ -thick gold cantilever beam suspended $3\ \mu\text{m}$ over a $300\ \text{nm}$ -thick gold drive electrode. A pair of dimples which are nominally $1.5\ \mu\text{m}$ deep are fabricated near the end of the cantilever beam to provide contact to the landing electrode. These dimples serve two important functions: (1) they provide standoff to prevent a short between the cantilever and the electrode, and (2) they minimize the contact area.

During operation, a bias voltage is applied between the cantilever beam and the drive electrode. When the magnitude of the bias exceeds a certain threshold called the pull-in voltage, the cantilever beam tip collapses onto the landing electrode closing the switch and reducing the resistivity. As the applied bias is further increased, another threshold is reached called electrode collapse. In this condition, the cantilever beam collapses onto the drive electrode, thus shorting the switch.

The switches were tested by wafer probing on a Cascade Summit 9000 Microprobe Station using standard microprobes. The bias is provided by an HP 3245A universal source. The output of the universal source is sent through a resistor and then to the probe input. Two HP 34401A multimeters are used to measure the bias at the probe input, and the resistance of the switch. Measurement of the switch resistance is done using a 4 point probe set up. All of the instruments are controlled by a PC using an IEEE-488 bus.

During testing, the applied bias from the source was swept from $5\ \text{V}$ to $75\ \text{V}$ in steps of $1\ \text{V}$. Over this range, all switches reached pull-in, and most switches collapsed. The switch is destroyed by the collapse, and thus only one sweep is made per switch. The software controlling the test records the applied bias (universal source setting), the measured voltage at the probe input, and the measured resistance of the switch.

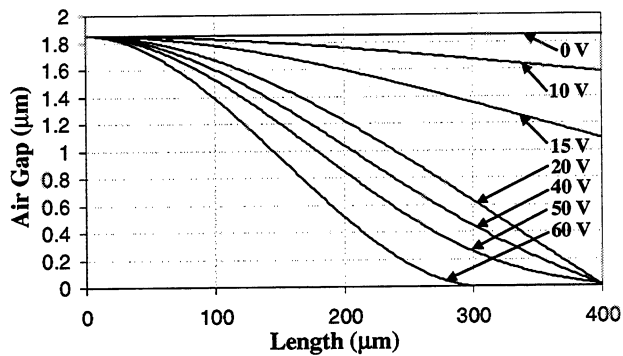


Figure 3: Simulated pull-in curves for a 75 μm -wide by 400 μm -long cantilever beam with an electrode width of 150 μm . The curves represent an applied bias ranging from 0 to 60 V. As shown, as the voltage is increased, the deflection of the cantilever beam also increases until collapse. This cantilever beam collapsed with an applied bias of 60 V and is shown in the figure.

4 RESULTS

Simulation results for a 75 μm -wide, 400 μm -long, and 4 μm -thick cantilever beam are plotted in Figure 3. The applied bias ranges from 0 V to 60 V as documented on the figure. The deflection curves show that as the applied voltage increases, the deflection of the cantilever beam also increases. For voltages 20 V through 50 V, the cantilever is pulled-in while at 60 V, the cantilever has collapsed onto the 'artificial dielectric'.

The data shown in Figure 4 was obtained from a switch similar to the one shown in Figure 2. The plot shows the measured drive bias and switch resistance as a function of applied bias. The two operational voltages can be found first as the point when contact is initiated (pull-in) and the resistance drops, and second as the point when the measured bias drops to zero (collapse). Once the pull-in is achieved, the resistivity gradually decreases from 1 Ω to approximately 0.7 Ω due to the increase in contact force of the switch. Once collapse occurs, the voltage drops to approximately zero and the resistivity increases rapidly. After the switch collapses, current flowing from the drive electrode and through the switch contaminates the four-point probe measurement.

To confirm that the measured voltage going to zero is due to collapse and not a surface breakdown, an optical profile was taken of two switches. The first was measured prior to any testing. The second was measured after it had been tested through collapse. The measured profiles of the two cantilevers are shown in Figure 5. The profiles were captured using a Burleigh Horizon interferometric microscope (IFM). As shown, the unactuated beam has a slight downward curl. This curvature follows the profile of the sacrificial layer that

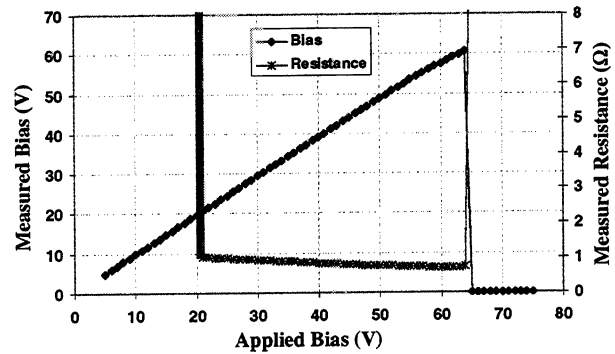


Figure 4: Measured bias and resistance curves for a switch similar to that shown in Figure 2 with an electrode width of 250 μm . The drop in the measured bias is primarily due to the collapse of the beam onto the drive electrode.

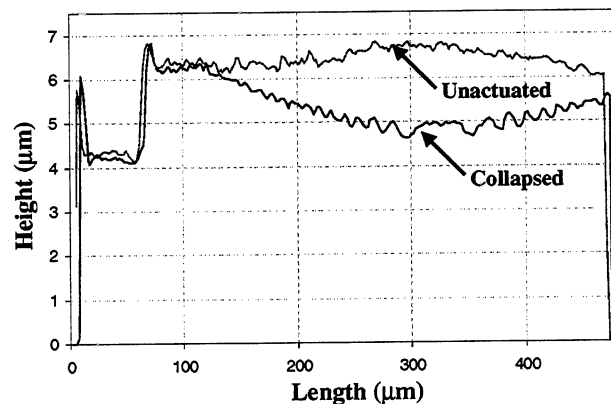


Figure 5: Measured beam deflections obtained using an interferometric microscope illustrating the unactuated and collapsed cantilever curvature for the beam. The unactuated beam has a slight downward curvature which is likely due to the underlying drive electrode while the collapsed beam has an upward curvature consistent with a device that pulled down onto the drive electrode.

conforms to the underlying electrode layer. The beam that has been collapsed clearly shows an upward curvature with the lowest point over the drive electrode. This profile is consistent with the beam having been collapsed.

Figure 6 shows the pull-in and collapse voltage levels for a series of 75 μm -wide by 400 μm -long beams with electrode widths ranging from 50 to 350 μm . For comparison, a simulation was done of the same set of beams. Nominal values were used for the beam width, length, and electrode width. The Burleigh IFM was used to measure the metal thickness (4.3 μm), dimple height

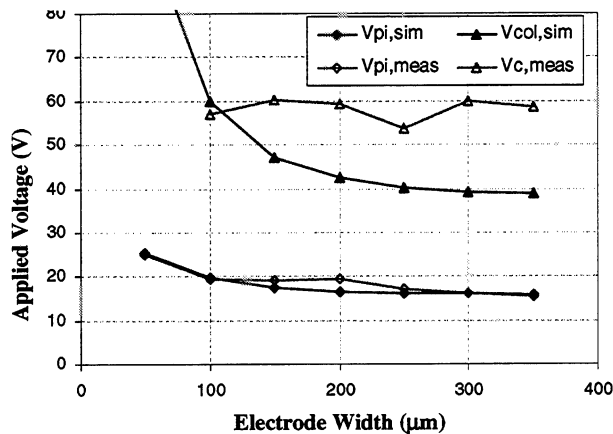


Figure 6: Simulated values of pull-in and release voltages for a gold beam with dimensions of $75 \mu\text{m}$ -wide, $400 \mu\text{m}$ -long, and $4.3 \mu\text{m}$ -thick. The beam is suspended $3.2 \mu\text{m}$ above the electrodes with a $1.2 \mu\text{m}$ deep dimple. Simulations are shown for electrode widths ranging from 50 - $350 \mu\text{m}$. In all cases, the position of the right side of the electrode remains fixed and the width is increased by moving the left side of the electrode. Measured pull-in and collapse voltages are shown for the average of 2 series of switches consisting of 7 beams with varied electrode widths. The $50 \mu\text{m}$ beam did not collapse at an applied bias of 75 V and is thus not plotted.

(1 - $1.5 \mu\text{m}$), and initial gap (3.0 - $3.2 \mu\text{m}$). The dimple height and initial gap were varied in the simulation to fit the pull-in voltage for the $350 \mu\text{m}$ wide electrode. The final values used were dimple height of $1.2 \mu\text{m}$ and initial gap of $3.2 \mu\text{m}$. Once these parameters were set, all simulations were run with the same numbers.

As illustrated, the simulated pull-in values correspond very well to the measured pull-in values. However, the simulated collapse voltages are significantly lower than the measured values. The discrepancy between measured and simulated collapse data is caused by two primary sources. First, the simulated beam is assumed to initially be perfectly flat; however, as shown in Figure 5 for an unactuated cantilever beam, the beam has a slight downward curl. This curl affects both pull-in and collapse voltages. Simulations done with an increased dimple height, and the same initial separation show almost identical pull-in voltages, but significantly higher collapse voltages. Secondly, the simulation does not take into account lateral forces. These lateral forces would result in a higher collapse voltage, but would not affect the pull-in voltage. As a final note, the data does show that the collapse voltage is much higher for low electrode widths, and relatively flat for electrode widths above $100 \mu\text{m}$.

5 CONCLUSION

The operating range of a series of metal-to-metal contact gold cantilever micro-switches were studied. The beam pull-in and collapse voltages were both measured and simulated with generally good agreement for the pull-in voltages over the $50 \mu\text{m}$ to $350 \mu\text{m}$ drive electrode widths. By determining the operating range, micro-switches can be operated above the pull-in voltage level but below the collapse level to increase the contact force and reduce the contact resistance. This decreased resistance is essential to providing high performance switches, and plays a significant role in the lifetime of the switch. Future measurements are focused on the validation of the pull-in and collapse voltage trends over a range of switch designs.

Acknowledgements: The authors gratefully acknowledge the efforts of AFRL/SND, Wright-Patterson AFB, Ohio, in developing the switch process and fabricating the switches used in this work. In particular, we thank Dr. Jack Ebel, Dr. Rick Strawser, Dr. Becky Cortez, and Dr. Kevin Leedy. This work was funded in part by the Air Force Office of Scientific Research.

REFERENCES

- [1] S. Majumder, N. McGruer, G. Adams, P. Zavracky, R. Morrison, J. Krim, "Study of contacts in an electrostatically actuated microswitch," *Sensors and Actuators A*, Vol. 93, No. 1, August 25, 2001, pp. 19-26.
- [2] D. Hyman and M. Mehregany, "Contact physics of gold microcontacts for MEMS switches," *IEEE Transactions on Components and Packaging Technology*, Vol. 22, No. 3, Sept 1999.
- [3] P. Osterberg and S. Senturia, "M-TEST: A test chip for MEMS material property measurement using electrostatically actuated test structures," *Journal of Microelectromechanical Systems*, 6 (2), 107-118, 1997.
- [4] M. Siegel, V. Maleev, and J. Hartman, "Mechanical design of machines," Fourth Edition, 71-85, 1965.